ORNL/TM-2019/1270

Modeling the IFR-1 Experiment: A BISON Metallic Fuel Benchmark

Kaylee M. Cunningham
Jeffrey J. Powers
Robert A. Lefebvre

July 2019

OAK RIDGE NATIONAL LABORATORY
MANAGED BY UT-BATTELLE FOR THE US DEPARTMENT OF ENERGY

ORNL/TM-2019/1270

Reactor Nuclear Systems Division

MODELING THE IFR-1 EXPERIMENT: A BISON METALLIC FUEL BENCHMARK

Kaylee M. Cunningham
Jeffrey J. Powers
Robert A. Lefebvre

July 2019

Prepared by
OAK RIDGE NATIONAL LABORATORY
Oak Ridge, TN 37831-6283
managed by
UT-BATTELLE, LLC
for the
US DEPARTMENT OF ENERGY
under contract DE-AC05-00OR22725

CONTENTS

LIST OF FIGURES

LIST OF TABLES

ACRONYMS

.csv	comma separated variable
1D	one-dimensional
2D	two-dimensional
2D-rz	2D axially symmetric
2D-rθ	2D radial-azimuthal
BOC	beginning of cycle
CW	cold worked
DOE-NE	US Department of Energy Office of Nuclear Energy
DU	depleted uranium
EBR-II	Experimental Breeder Reactor-II
EFPD	effective full power day
EOC	end of cycle
FEM	finite element method
FFTF	Fast Flux Test Facility
FIMA	fissions per initial metal atom
GUI	graphical user interface
IFR	Integral Fast Reactor
LHGR	linear heat generation rate
MOOSE	Multiphysics Object Oriented Simulation Environment
NEAMS	Nuclear Energy Advanced Modeling and Simulation
NRC	US Nuclear Regulatory Commission
ORNL	Oak Ridge National Laboratory
PIE	post-irradiation examinations
VTR	Versatile Test Reactor

1. INTRODUCTION

As the 1970s nuclear reactor fleet slowly begins the decommission process, the US Department of Energy Office of Nuclear Energy (DOE-NE) aims to stimulate and support the construction and implementation of new nuclear reactors across the country in hopes of continuing the generation of clean, reliable, resilient energy. As a result, various efforts have been introduced to accelerate this process, including the Versatile Test Reactor project (VTR) and the Nuclear Energy Advanced Modeling and Simulation (NEAMS) program.

1.1 VERSATILE TEST REACTOR (VTR)

The Versatile Test Reactor (VTR) is a new fast spectrum test reactor that is currently being developed in the United States under the direction of the US Department of Energy, Office of Nuclear Energy [1]. The VTR mission is to enable accelerated testing of advanced reactor fuels and materials required for advanced reactor technologies. This includes neutron irradiation capabilities which would support testing under alternate coolants including molten salt, lead/lead-bismuth eutectic mixture, gas, and sodium. The VTR aims at addressing most of the needs of the various stakeholders, primarily composed of advanced reactor developers, as well as a number of others interested parties. Design activities are underway at multiple national laboratories targeting a first criticality date by 2026, with General Electric-Hitachi joining the project to contribute to the VTR plant design. Current efforts are focused on all aspects of the VTR design.

The current proposed VTR concept is a 300 MWth sodium-cooled pool type reactor with metallic alloy fuel.

1.2 NUCLEAR ENERGY ADVANCED MODELING AND SIMULATION (NEAMS)

The NEAMS program is advancing modeling and simulation efforts focused on developing new tools to analyze and optimize the performance and reliability of existing and advanced nuclear power plants. NEAMS is developing computational tools that allow researchers to shed light on current problems and new ideas in unique ways that were previously considered impractical due to their excruciating detail. NEAMS can enhance understanding in areas ranging from changes in nuclear fuel materials to full-scale power plant operations [2].

The NEAMS mission is to develop, apply, deploy, and support state-of-the-art predictive modeling and simulation tools for design and analysis of current and future nuclear energy systems. This is accomplished by using computing architectures ranging from laptops to leadership-class computer facilities. The tools in the NEAMS ToolKit will enable transformative scientific discovery and insights otherwise not attainable or affordable and will accelerate the solutions to existing problems, as well as deployment of new designs for current and advanced reactors [2].

2. BACKGROUND

This report documents work performed at Oak Ridge National Laboratory (ORNL) to develop a two-dimensional computational model of a U-19Pu-10Zr fuel pin from the IFR-1 metallic fuel experiment performed in the Fast Flux Test Facility (FFTF) in 1985. This model was created using the BISON fuel performance modeling code through a new platform developed by NEAMS known as *Workbench*. This model was generated to benchmark the BISON code for metallic fuel analysis.

2.1 METHODS

BISON was set up remotely through NEAMS Workbench on a Windows machine and was used to generate this model.

2.1.1 NEAMS Workbench

The NEAMS Workbench is a software being developed to facilitate the transition from conventional to high-fidelity computational tools by providing a common user interface for model creation, review, execution, output review, and visualization for integrated codes [2].

The NEAMS Workbench can use common user input, including engineering-scale specifications, that are expanded into application-specific input requirements using customizable templates. The templating process enables multi-fidelity analysis of a system from a common set of input data. Additionally, the common user input processor can provide an enhanced alternative application input that provides additional conveniences over the native input, especially for legacy codes. The various integrated codes and application templates available in NEAMS Workbench broaden the user community and facilitate system analysis and design [2].

Ultimately, the NEAMS Workbench improves usability and streamlines the process of utilizing the BISON tool, locally and remotely. The software consists of an advanced text editor that incorporates input validation as well as auto-completion. Also available in the application's graphical user interface (GUI) data plotting to assist the user with analysis of input and output data. Through these capabilities the NEAMS Workbench provides a common analysis environment that aids in accelerating the user's adoption of advanced computational tools, such as BISON.

2.1.2 BISON

The BISON fuel performance code is a finite element method (FEM)-based software tool being developed by various organizations and led by the Idaho National Laboratory for DOE-NE. BISON is based on Idaho National Laboratory's Multiphysics Object Oriented Simulation Environment (MOOSE). The code can simulate a host of fuel and cladding compositions and geometries, including light-water reactor fuel rods, TRISO particle fuel, metallic rod, and plate fuel. Depending on the problem type and complexity level, varying dimensionality can be used in BISON, including one-dimensional (1D), 1.5D, 2D axially symmetric (2D-rz), 2D radial-azimuthal (2D-rθ), and 3D models. Visualizations can be created through third-party software such as Paraview or VisIt using the results stored in output Exodus files. BISON calculations include temperature- and burnup-dependent thermal properties, fission product swelling, thermal and irradiation creep, fission gas production and release, irradiation-induced swelling, and other phenomena [3].

For this model, BISON was used to analyze a U-19Pu-10Zr ternary metallic fuel alloy. This fuel composition is very similar to a proposed U-20Pu-10Zr driver fuel concept for VTR.

2.1.3 Integral Fast Reactor (IFR)-1

The IFR-1 experiment included irradiation of three fuel slug compositions: U-10Zr, U-8Pu-10Zr, and U-19Pu-10Zr. All were clad in 20% cold-worked (CW) D9. Of the 169 fuel pins in the IFR-1 experiment, 18 were U-19Pu-10Zr, 19 were U-8Pu-10Zr, and 132 were U-10Zr. The experiment was conducted in 1985 at the FFTF. The first of these irradiation tests performed at FFTF was IFR-1, which included 169 wire-wrapped, sodium-bonded, full length (91.4 cm active fuel column height) metallic fuel elements. IFR-1 fuel pins contained axial blankets of depleted uranium (DU) U-10Zr that were 16.5 cm long and were

situated above and below the main fuel column [6]. Post-irradiation examinations (PIE) demonstrated clear resemblance to short-pin (34.3 cm active fuel column height) experimentation of similar material composition that was performed at the Experimental Breeder Reactor-II (EBR-II) [4].

3. IFR-1 MODEL

ORNL stitched together information collected from various sources to construct a 2D-rz model of a generalized U-19Pu-10Zr fuel pin from the IFR-1 experiment.

3.1 GEOMETRY AND MATERIALS

The model was created according to the geometric input parameters specified in Table 1 below. The EBR-II x441 experiment model input file (x441.i), which is available in the BISON repository, was used as a starting template. A few IFR-1 input parameters have yet to be determined, but given the similarities between the IFR-1 experiment and the x441 EBR-II experiment, the values for missing IFR-1 parameters have been temporarily defined using values from the x441.i input file as rough estimates.

3.1.1 Dimensions

Table 1 summarizes the dimensional input parameters used in the IFR-1 BISON model, along with the source of each parameter value and the line number on which that parameter can be found in the current IFR-1 BISON model.

Table 1. Dimensional Input Parameters with Sources

Parameter	Value	Source	Input file line number
Slug outer radius	2.490 mm	[5, pg. 47][1]	31
Initial Na bond gap thickness	0.380 mm	derived	34
Cladding thickness	0.560 mm	[5, pg. 47]	30[2]
Rod diameter	6.86 mm	[5, pg. 47]	517
Rod pitch	8.230 mm	[5, pg. 47][3]	518
Fuel slug height	91.40 cm	[5, pg. 47]	32
Plenum height	106.2 cm	[6, pg. 125]	33
End-plug thickness	2.240 mm	[x441.i]	35
Gap between slug bottom and end-plug top	0.310 mm	[x441.i]	36

Parameters such as *rod diameter* and *rod pitch* were not explicitly defined in the literature; in such cases, footnotes are included herein to provide further detail on how these values were derived from source(s) cited.

[1] The radius is not explicitly stated; the reference provides the slug's outer diameter, which was used to derive the radius value listed.
[2] All line number references in the text of this report refer to line numbers in Appendix A.
[3] Pitch is not explicitly stated; however, the source defines the outer diameters of the pin and wire. Reference [1] provides a photo (page 111) of the fuel bundle illustrating a single wire between neighboring rods, with neighboring wires offset axially. Therefore, pitch equates to the sum of the wire's outer diameter to the pin's outer diameter. These values were added to obtain rod pitch.

3.1.2 Mesh

A customized smeared pellet mesh was generated through the BISON input file using a QUAD8 element type from libMesh. In the mesh, 6 fuel elements were defined in the radial direction, while 260 were defined in the axial direction. Cladding consisted of 4 elements defined in the radial direction and 260 in the axial direction, along with 3 radial elements in the upper end plug and 1 axial element in the lower end plug. Future work should perform, and document, a mesh optimization study to more explicitly balance accuracy and calculation runtime. A centroid partitioner was specified with a sort in the y direction. Patch size, or the number of nodes considered in the NearestNode neighborhood, was set to 50, and the update strategy was set to *automatic* (see Figure 1).

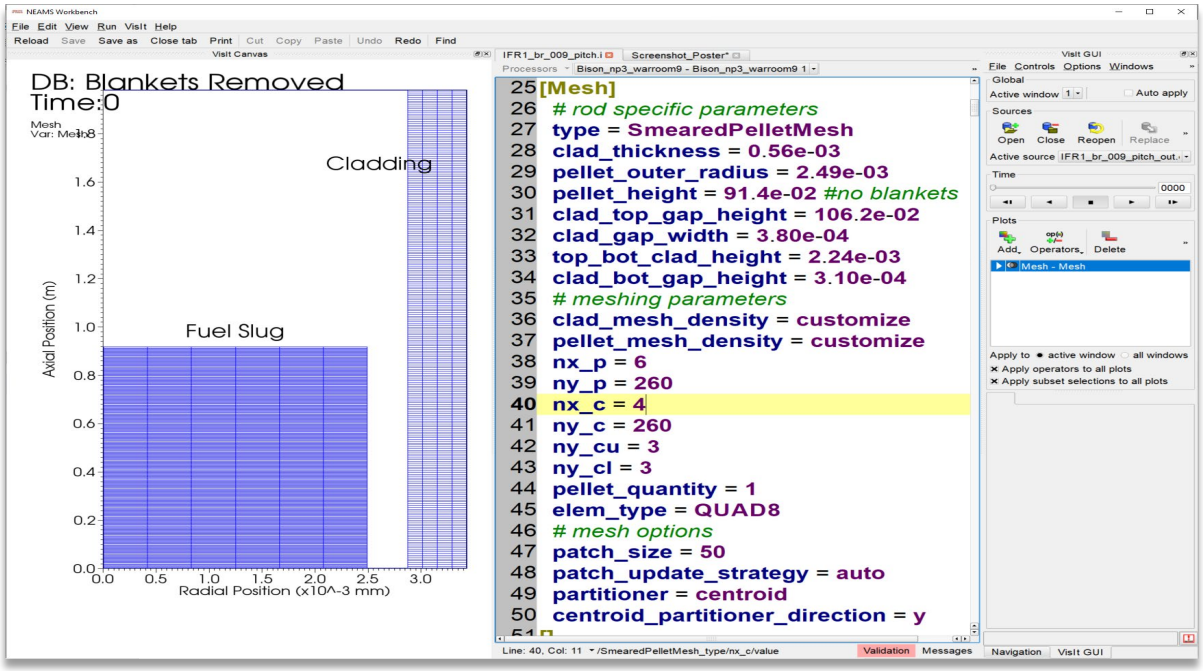

Figure 1. Screenshot of mesh visualization (left), BISON input meshing parameters (center), and VisIt graphical user interface (GUI) (right) all within the NEAMS Workbench.

3.1.3 Materials

The materials used in the IFR-1 experiment included a U-19-Pu-10Zr ternary alloy fuel clad in 20% CW D9. To replicate this, the molar fractions within the input file were set to x_Pu = 0.19 and x_Zr = 0.10 in four different places (lines 531–532, 538–539, 546–547, 587–588). Modeling the D9 cladding proved difficult because D9 material models are not currently included in BISON. HT9 cladding materials were used for now, but IFR-1 model should be updated when D9 material models are added to BISON.

As a simplification, the DU U-10Zr axial blankets were not included in this initial model. Limitations in BISON's internal mesh generation script prevent modeling two different fuel slug types in a single mesh; this simplification of ignoring the U-10Zr axial blankets therefore avoids the need to use external mesh generation resources. As a result, this modeling approximation ignores mechanical and thermal impacts of the blankets by assuming that all power production occurs in the main fuel column. This should be conservative for thermal analysis due to concentrating power production into a smaller region. The mechanical impacts of this approximation should be small and are considered acceptable for this baseline model [7]. This document therefore primarily focuses on this initial baseline model, with no axial blankets. However, a study performed comparing an approximation to simulating the blankets will be

explored in Section 5. Additional options are also being investigated to explicitly model the axial blankets, including possible use of mesh modifiers in BISON or external mesh generation tools.

3.2 OPERATING CONDITIONS

Determining operating conditions for the BISON model input file required a detailed search through the literature, as well as drawing from the information recorded to indirectly calculate required parameter values that were not stated explicitly. In particular, calculations were performed to determine power functions, time steps, and flux, while coolant parameters were mostly assembled from various sources within the literature.

3.2.1 Power Functions

BISON input requires that certain functions be defined with corresponding time steps: specifically linear heat generation rate (LHGR) and axial power peaking factors. Obtaining input data for time, LHGR, and axial power required literature examination, as well as subsequent calculations.

3.2.1.1 Time

BISON requires that power function data have respective corresponding time steps defined in a list as the *x* variable for linear functions (lines 158, 165, and 172)[4]. In line 188, because axial power is a bilinear function, time is the *y* variable.

Appendix A, "Detailed Pin and Assembly Composition, Flow and Power Characteristics," in Porter and Tsai's *Full-length Metallic Fast Reactor Fuel Pin Test in FFTF* [4], includes a table detailing the time cycles for IFR-1. Effective full power days (EFPDs) are listed for each cycle. Page 67 in the same document [4] lists the cycles as 9A, 9B, 9C, 10A, 10A-2, and 10B. However, page 65 includes an inconsistency in cycle names, listing them as: 9A-1, 9A-2, 9B, 10A-1, 10A-2, 10A-3, 10A-4, and 10B. Consequently, cycle 9A-2 from this table (page 65) was assumed to be 9B; 9B was assumed to be 9C; 10A-1 to be 10A; 10A-2, 10A-3, and 10A-4 were added together and assumed to be 10A-2, and 10B remained 10B. These assumptions were made based on the remainder of the Appendix A [4] cycle references and notes included with the table. After the specified cycle durations (in EFPDs) were summed, each cycle's total duration (in EFPDs) was multiplied by 86,400 to convert them to seconds (3,600 s/hr × 24 hr = 86,400 s). Cumulative duration was then calculated for each point in time. One hour (3,600 s) was added between cycles to separate time steps and to smooth calculations within BISON. This process resulted in the list of time steps provided in Table 2.

Table 2. Time Step Calculations

Cycle	Time per cycle (EFPDs)	Calculation	Time (s)
0	N/A	0 =	0
9A BOC	N/A	0+3600 =	3,600
9A EOC	29.4	(29.4 × 86400) + 3600 =	2,543,760
9B BOC	N/A	2543760 +3600 =	2,547,360
9B EOC	108.3	(108.3 × 86400) + 2547360 =	11,904,480
9C BOC	N/A	11904480 + 3600 =	11,908,080
9C EOC	97.7	(97.7 × 86400) + 11908080 =	20,349,360
10A BOC	N/A	20349360 + 3600 =	20,352,960

[4] For all line number references, see Appendix A.

10A EOC	66.3	(66.3 × 86400) + 20352960 =	26,081,280
10A-2 BOC	N/A	26081280 + 3600 =	26,084,880
10A-2 EOC	85.5	(85.5 × 86400) + 26084880 =	33,472,080
10B BOC	N/A	33472080 + 3600 =	33,475,680
10B EOC	126.7	(126.7 × 86400) + 33475680 =	44,422,560

3.2.1.2 LHGR

For BISON to determine LHGR (`[./power_history]` on line 156), *x* and *y* variables must be defined. In this case, *x* is the time in seconds mentioned previously, and *y* is LHGR in units of W/m.

To stitch together a plot of the two variables, information was again obtained from Appendix A of Porter and Tsai's 2011 document [4]. In particular, Table 1 on page 93 contains a list of peak axial pin powers for 181### pins as determined by Westinghouse. Pin 181193, (listed as 193 in the pin column) is the only U-19Pu-10Zr pin destructively examined [4, pg. 1]; the beginning of cycle (BOC) and end of cycle (EOC) LHGRs are listed in units of kW/ft for six FFTF operating cycles. These values were recorded in a spreadsheet. The BOC and EOC LHGRs for each cycle were then converted from kW/ft (given units) to W/m (required units for BISON). Table 3 below summarizes this information.

Table 3. LHGR's Per Cycle with Converted Units

Cycle	9A	9B	9C	10A	10A-2	10B
BOC (kW/ft)	13.94	12.33	12.14	10.86	10.06	9.80
EOC (kW/ft)	13.14	11.65	11.66	10.86[5]	9.14	9.66
BOC (kW/m)	45.7232	40.4424	39.8192	35.6208	32.9968	32.1440
EOC (kW/m)	43.0992	38.2120	38.2448	35.6208	29.9792	31.6848

The LHGR values were listed chronologically for the y input in `[./power_history]` (line 160). Figure 2 shows the time-dependent LHGR history as reconstructed and used in BISON for this pin, with time converted to days to enhance clarity and understanding.

[5] No EOC LHGR was listed, so 10.86 was used for BOC and EOC.

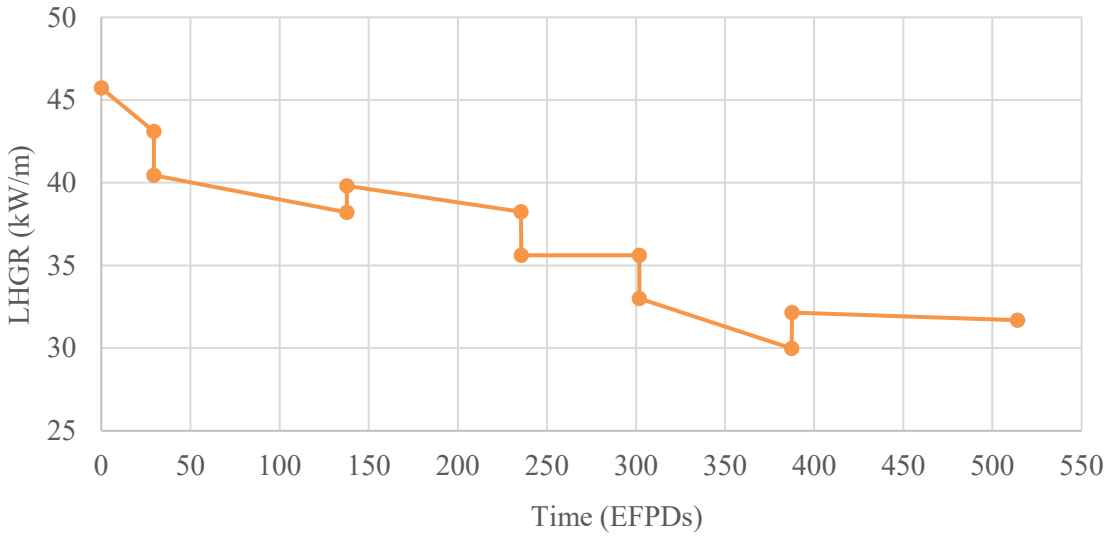

Figure 2. LHGR piecewise linear history reconstructed for IFR-1 U-20Pu-10Zr fuel pin over its operating lifetime.

3.2.1.3 Axial Power

Axial power distribution is required for the BISON input (`[./axial_peaking_factors]` line 177) and was also determined from Appendix A in Porter and Tsai's 2011 document [4]. On page 101, a figure displays local power and temperature as a function of axial position for IFR-1 pin 181193. Relative axial position is indicated as *x/L* in that figure and in this work, where *x* is the local axial height, and *L* is the total active fuel height of the pin. Focusing on the axial power curve, a web-based data extraction tool was used to pull points from the plot and export them into a comma-separated variable (.csv) file that was opened in a spreadsheet.

All positions in x/L were then multiplied by 0.914 m, which was the length of the active fuel column, to covert to axial position in meters; these products were listed as the *x* variable (line 179) in `[./axial_peaking_factors]`. The same time steps (see Section 3.2.1.1) were listed to define the *y* variable (line 188), which is time. All powers extracted were then converted from units of kW/ft to kW/m. These values were averaged to calculate a pin-average LHGR. Each individual local axial power was divided by the calculated pin-average LHGR to produce a height-dependent local relative power. The resulting list of relative powers was entered in a repeating list for the z variable (line 192). All of this axial power information is summarized in Table 4.

Table 4. Axial Power Input Parameters

x/L	Power (kW/m)
0.0009	16.862571
0.00763	19.431812
0.0137	22.061049
0.05058	25.219242
0.10088	29.868338
0.14982	33.381704
0.20077	37.073859
0.25038	40.347839

0.30065	42.664878
0.35023	44.025375
0.40047	44.727912
0.44066	44.895286
0.45071	44.892282
0.50027	44.279499
0.55049	43.307739
0.6007	41.498829
0.6509	38.972363
0.70042	35.848134
0.7506	32.125741
0.80012	28.463344
0.85096	24.082991
0.90047	19.882427
0.95064	15.382682
0.96937	13.403795
0.97938	10.47077
0.98605	8.1367096
0.99204	5.6832568
0.99938	3.647978

3.2.2 Flux

BISON requires a *flux factor*, which is a ratio of flux to power in units of $\frac{\mathrm{n/cm^2-}s}{\mathrm{W/m}}$. Determining this fast flux factor for the `[./fast_flux]` block within the materials block (line 620) required calculations based on values Porter and Tsai's 2011 document [4]. On page 2 [4], the EOL fast fluence of IFR-1 was defined as 15.6×10^{22} n/cm^2. This EOL fast fluence was divided by the previously calculated EOL time (see Section 3.2.1.1, Table 2) to calculate an average fast flux of 3.5×10^{15} n/cm^2-s, as shown in Eq. (1) below.

$$\frac{15.6 \times 10^{22} \frac{n}{cm^2}}{44422560s} = 3.5 \times 10^{15} \frac{n}{cm^2 - s} \tag{1}$$

The lifetime average LHGR, an average of all BOL and EOL LHGR values listed in Table 3, was calculated to be approximately 37,000 W/m. The lifetime-average fast flux (3.5×10^{15} n/cm^2-s) was divided by this lifetime-average LHGR (37,000 W/m) to produce a flux factor of $9.5 \times 10^{10} \frac{\mathrm{n/cm^2-s}}{\mathrm{W/m}}$. As shown in Eq (2), this was converted from cm^2 to m^2 to calculate the final flux factor used for the BISON input of $9.5 \times 10^{14} \frac{n/m^2-s}{W/m}$.

$$\begin{aligned} \frac{3.5 \times 10^{15} \frac{\mathrm{n}}{\mathrm{cm^2 - s}}}{37000\ \mathrm{W/m}} &= 9.5 \times 10^{10} \frac{\mathrm{n/cm^2 - s}}{\mathrm{W/m}} \times 10^4 \frac{\mathrm{cm^2}}{\mathrm{m^2}} \\ &= 9.5 \times 10^{14} \frac{\mathrm{n/m^2 - s}}{\mathrm{W/m}} \end{aligned} \tag{2}$$

3.2.3 Coolant

Coolant parameters were mostly determined from the literature. The coolant temperature ramp required for the functions block—`[./coolant_temp_ramp]` line 170—was defined as a constant temperature at each time step. That temperature was obtained from the literature [8] as 360 °C and converted to Kelvin (633 K). This was input for the *y* values, except for the first and last time steps in line 167. The first time step is set at room temperature (298 K), and the last is a decrease of roughly 50% in temperature (350 K).

However, some parameters have not yet been found. Specifically, values for the coolant pressure ramp function block (`[./coolant_press_ramp]` line 163) could not be determined. Given the similarities between EBR-II and FFTF, the coolant pressure value from the x441 BISON input (0.151 MPa) is used in this IFR-1 model for now should be sufficient. The inlet mass flux (in units of $\frac{\mathrm{kg}}{\mathrm{m^2{-}s}}$) required for the coolant channel block in BISON (`[./convective_clad_surface]` line 515) has also been unobtainable thus far. For now, the value from the x441 BISON model (5261.5 $\frac{\mathrm{kg}}{\mathrm{m^2{-}s}}$) is used in this IFR-1 model, although this is almost certainly at least slightly inaccurate. Temperature values, especially for cladding, may be consequently skewed. As soon as a more accurate inlet mass flux can be calculated or obtained, the model must be updated and adjusted accordingly.

4. RESULTS

Numerous simulations were performed to generate visualizations of various parameters of interest and to develop detailed analyses comparing documented IFR-1 experimental results to the results from this BISON model. Specifically, burnup and temperature were compared directly to IFR-1 experimental data.

4.1 GENERAL OUTPUT

Table 5 below summarizes the BISON model's most essential parameters at EOL that are of interest to the VTR project and potentially to the general nuclear community.

Table 5. BISON Model Output Data

Parameter	Value
Peak fuel temperature (at 138 d)	1,160 K
Peak cladding temperature (at 1 hr)	955 K
Maximum average fuel surface temperature during operation (at 1 hr)	867 K
Maximum average inner cladding temperature during operation (at 1 hr)	897 K
EOL average burnup	6.5 %
EOL peak burnup	8.7 %
EOL plenum pressure	3.9 MPa
EOL maximum hoop stress	63 MPa
EOL maximum cladding creep strain	5.33 × 10-4
EOL fission gas release	92.3 %
EOL maximum cumulative damage fraction	8.60×10^{-4}

The maximum hoop stress of approximately 63 MPa occurred 0.51 m from the bottom of the active fuel column (x/L = 0.6). The peak burnup of 8.7% fissions per initial metal atom (FIMA) was achieved 0.42 m above the bottom of the active fuel column (x/L = 0.5) [7]. Gap thickness, as illustrated in Figure 3,

decreases as burnup progresses until fuel and cladding come into contact. Results for this model indicate gap closure (fuel-cladding contact) occurs at roughly 6.6% average burnup; however, past experiments indicate the gap should close sooner, so this requires further investigation.

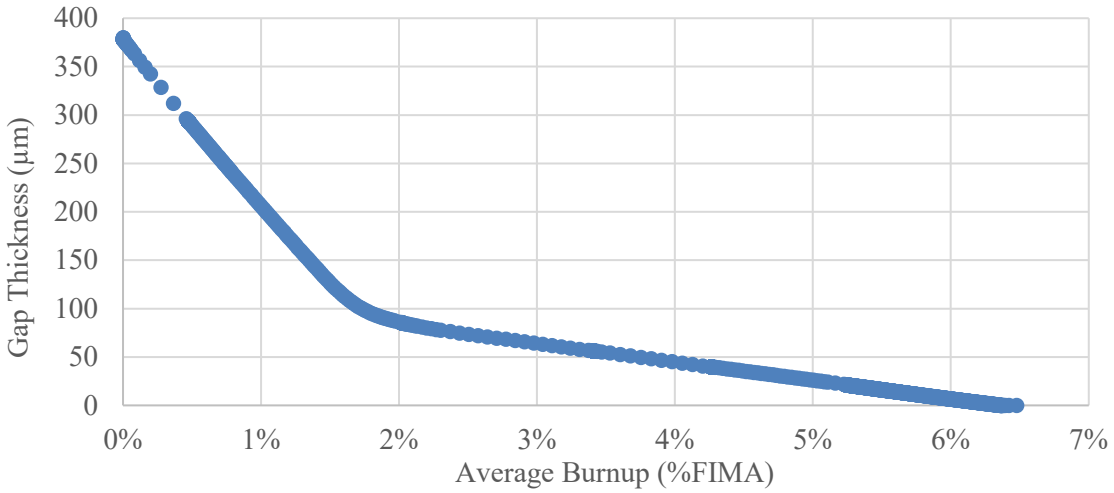

Figure 3. Scatter plot of model's gap thickness (in micrometers) across average burnup (in % FIMA).

Collectively, these output values produced by the IFR-1 BISON model generally meet the qualitative behavior expectations.

4.2 TEMPERATURE

Temperature was expected to be slightly skewed due to the incorrect inlet mass flux value used in the input file. Generally, this was demonstrated in the following results. The overall temperature distribution (Figure 4) and the average fuel centerline temperature (Figure 5) appear to be qualitatively reasonable. Figure 4 shows the average fuel centerline temperature peaks in the middle of the fuel slightly above the center, as expected, and then decreases radially and axially as heat is conducted outward and fission rates also decrease. The cladding temperature distribution follows the coolant temperature distribution axially, with lower temperatures near the inlet at the bottom and higher temperatures near the outlet at the top, while also exhibiting the expected slightly higher temperature at cladding inner surface that decreases radially outward through the cladding.

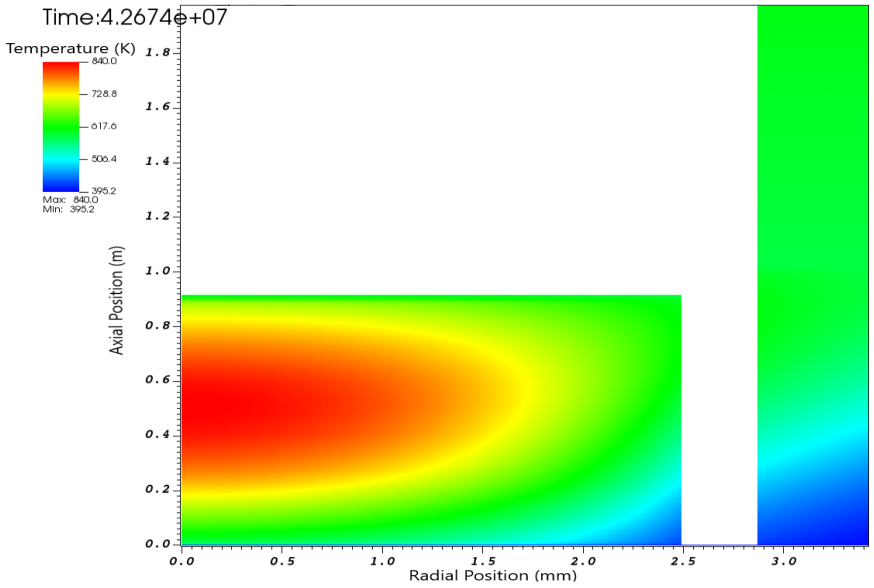

Figure 4. BISON IFR-1 model temperature distribution visualization generated in NEAMS Workbench's VisIt GUI.

The average fuel centerline temperature illustrated in Figure 5 shows trends demonstrating two main effects overlaid on top of each other: time-dependent variations in rod-average LHGR as well as burnup-dependent changes in fuel thermal conductivity. Time-dependent changes in the rod-average LHGR directly impact the fuel temperature, as portrayed by the discontinuities in Figure 5. They occur when the power history curve in Figure 2 shows the same discontinuities. At the same time, the overall shape of the results in Figure 5 follow the burnup-dependent evolution of fuel thermal conductivity during irradiation of UPuZr metal fuel; the fuel thermal conductivity starts out highest in the fresh fuel, decreases during irradiation until hitting a minimum fuel thermal conductivity around 2 %FIMA which is when fuel temperature peaks, and then slightly recovers some thermal conductivity as burnup progresses to around 5 %FIMA.

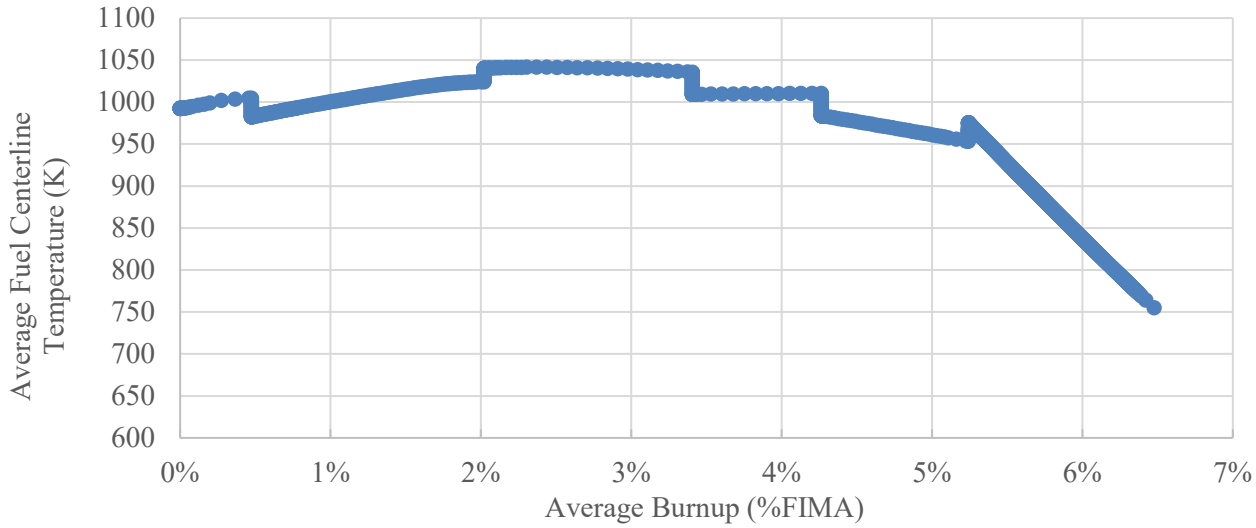

Figure 5. Scatter plot of IFR-1 model average fuel centerline temperature (K) as a function of average burnup (%FIMA).

The cladding's inner temperature (Figure 6) illustrates the expected error; the model results generally follow the same behavioral trends as the experimental data, but they are approximately 25 K higher. This indicates a possible consistent bias in the model which could be resolved with improved coolant inlet conditions.

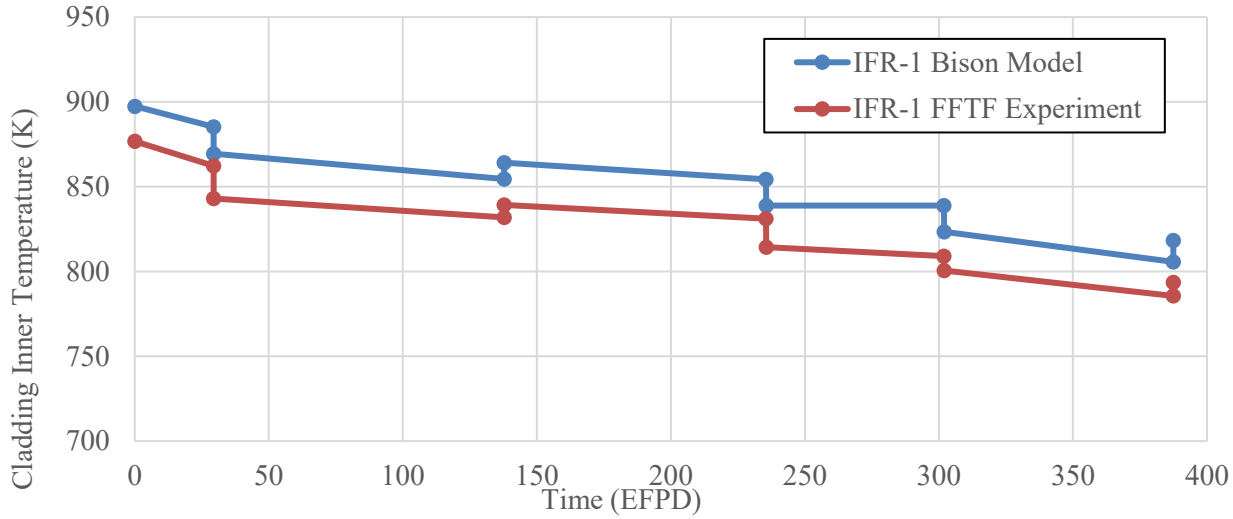

Figure 6. Connected scatter plot comparing cladding inner temperatures (K) over time (EFPDs) between the BISON IFR-1 model and IFR-1 experimental values obtained from Porter and Tsai, 2011 [4][6].

The EOL average fuel surface temperature produced was 563 K, while the EOL average inner cladding temperature was 580 K. This created initial concern because the cladding temperature should be lower than the fuel temperature. However, the radial temperature distributions shown in Figure 7 across the axial center of the pin (x/L = 0.5) for several points in time show reasonable radial temperature distributions. The EOL average inner cladding temperature being higher than the EOL average fuel

[6] The experimental values from Porter and Tsai [4] are found in the figure on page 100. The temperatures used were converted from Celsius to Kelvin by adding 273 to each value.

surface temperature is therefore most likely a result of the approaches used to calculate those average values; the cladding is taller than the fuel height, so low temperature conditions near the coolant inlet matter less in the cladding than in the fuel. When comparing fuel and cladding average temperatures in the future, it would be best to average them over the same axial region (active fuel length) to enable direct comparisons, in addition to calculating a true (full-height) axially-averaged cladding temperature if desired.

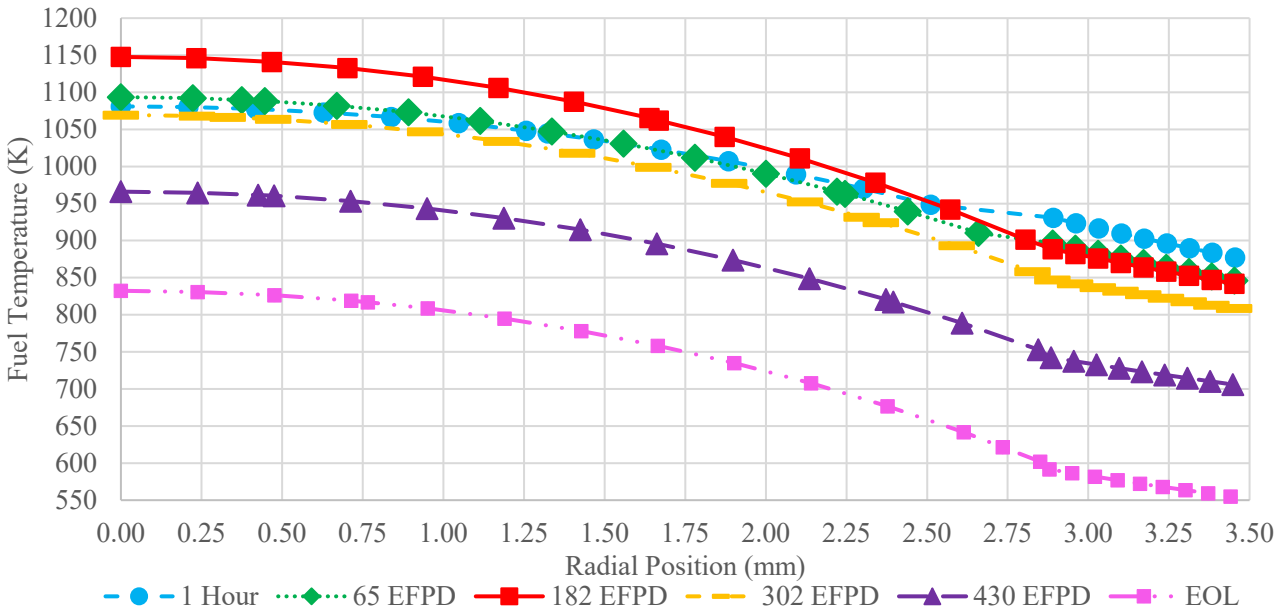

Figure 7. Radial temperature distribution of the IFR-1 BISON model throughout the pin's life cycle.

4.3 BURNUP

Burnup results from the BISON model compared very well against past work, within 5% relative error. The distribution (Figure 8) illustrates the peak of 8.7% occurring at roughly 0.42 m (x/L = 0.5), as previously mentioned; this location of the peak burnup needs to be examined.

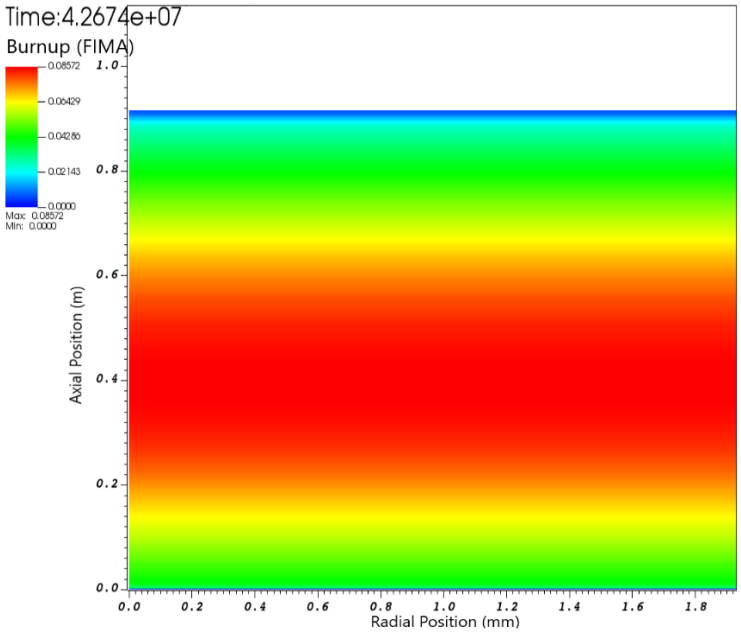

Figure 8. BISON IFR-1 model overall burnup distribution visualization generated in NEAMS Workbench's VisIt GUI.[7]

Relative errors were calculated for each cycle for which experimental data were available, as shown in Table 6. Given the difficulty in directly measuring burnup or indirectly inferring burnup using destructive assay to measure quantities and ratios of certain isotopes, this experiment result is in effect a previous result from neutronics calculations. Relative errors were calculated by subtracting the actual value from the simulation value and then dividing that quantity by the simulation value. The average relative error across the cycles was 2.91%. The burnup values are also illustrated in Figure 9, further showing the small relative error.

Table 6. IFR-1 Experiment and BISON Model Burnup Results and Relative Errors

Cycle	Time (EFPD)	Experimental peak EOL burnup (%FIMA) [4]	BISON model peak EOL burnup (%FIMA)	Relative % error
9A	138	2.61%	2.67%	2.3%
9B	244	4.44%	4.67%	5.2%
9C	342	6.12%	6.27%	2.4%
10A1	408	7.18%	7.26%	1.1%

[7] The cladding is not visible in this figure because burnup only occurs in the fuel region.

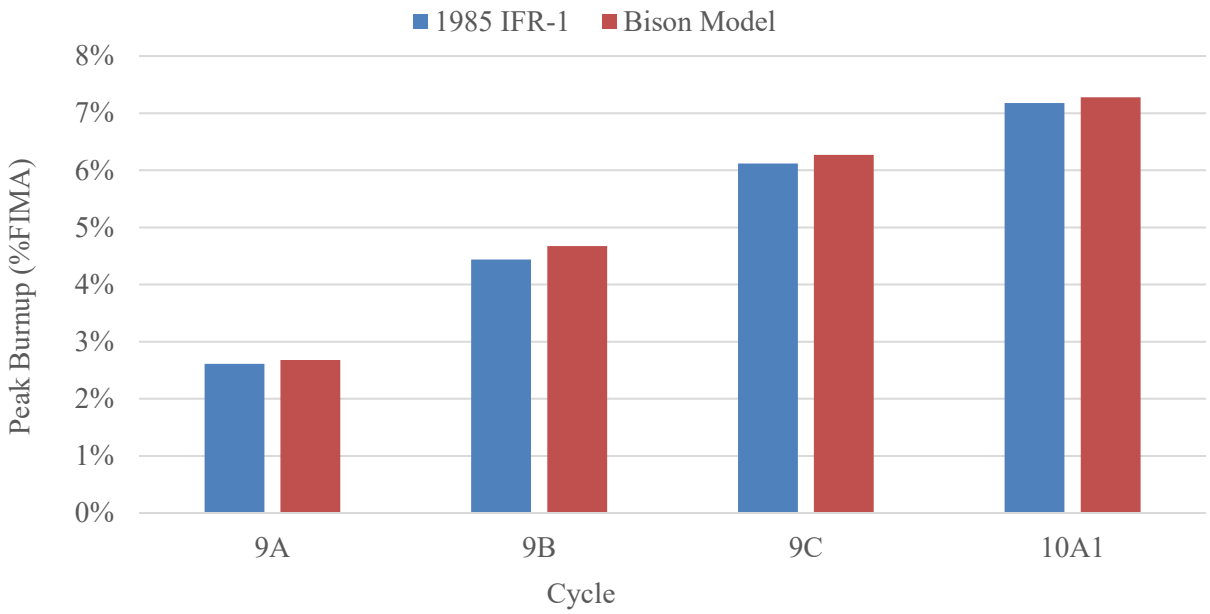

Figure 9. Comparison of burnup results between IFR-1 experiment (Porter and Tsai, 2011 [4], pp. 84–87, Appendix A) and BISON model.

5. DISCUSSION: U-10ZR AXIAL BLANKETS

As previously mentioned, the IFR-1 experiment contained 16.5 cm U-10Zr axial blankets above and below the active fuel column. The reference model developed for this effort used a modeling approximation of ignoring these axial blankets, as discussed in Section 3.1.3. However, an additional variant of the IFR-1 BISON model was created to approximate the impact of including these blankets. For this BISON model, the blanket regions were added and modeled as U-19Pu-10Zr (the same as the active fuel), and then the axial power distribution was defined to reduce the relative power for the first and last six values to 0.1. The height of the active fuel was extended to 124.4 cm to accommodate the blanket addition. These changes in the BISON input model are shown below.

```
[Mesh]
pellet_height = 124.4e-02 # blankets
[]

[./axial_peaking_factors]
x = ' 0 0.000821953…0.913433187' # axial length, 29 points
y = '0 3600…44422560' # time in seconds, 13 points
z = '0 0.1 0.1 0.1 0.1 0.1 0.1 1.09186242 1.18828444 1.25652355
1.29659156 1.31728199 1.32221131 1.32212284 1.30407578
1.27545645 1.22218224 1.14777528 1.05576358…0.7092683 0.1 0.1
0.1 0.1 0.1 0.1 0.1’ # relative power, 13x29 points
[../]
```

The goal of this model with the blankets included was to assess the impact of minimal power production within the top and bottom blanket portions of the fuel. This produced a significantly lower burnup percentage, reaching a maximum of 6.7 % FIMA. Given the overall decreased accuracy resulting from

approximations and the increased complexity of this model, the primary focus of this report remains the model only, including the active fuel column.

6. CONCLUSIONS

A two-dimensional (2D) axisymmetric model of the 1985 IFR-1 experiment performed at FFTF was successfully created and executed on a remote computational resource through the NEAMS Workbench to provide a metallic fuel analysis benchmark model in support of the VTR project using the BISON fuel performance code. Results from analysis performed using this initial model agree well with a couple burnup and temperature calculations shown in the literature that used other codes, which provides some confidence that this initial model used accurate input parameters and boundary conditions.

6.1 FUTURE WORK

Some areas of this model need improvement.The current IFR-1 benchmark model only includes the active fuel column. To improve the accuracy of this model, generating a more accurate model that includes axial blankets could prove useful. Current coolant parameter assumptions, particularly the incorrect inlet mass flux approximation, should also be addressed and updated to the correct FFTF values if these values can be obtained. This model would also benefit from additional capabilities in BISON, specifically material models for D9 cladding. Addressing the modeling limitations reached would not only improve this model, but would also increase BISON's versatility, thereby enhancing its usability for future metallic fuel models.

Future work should also compare results from the IFR-1 benchmark model against post-irradiation exanination (PIE) data gathered from non-detsructive or destructive analysis of the IFR-1 experiment pins. Comparisons against any in-pile measurements that can be found, in any exist, would also be beneficial.

Finally, a BISON input can contain duplicate parameters and difficult syntax constructs. An improved BISON input interface will be initiated using the NEAMS Workbench's analysis sequence processor capabilities [9] to remove duplicate input and restrictive syntax, thus enhancing usability for new users. Additionally, the new interface will automate and streamline the BISON analysis workflow. The overarching goal of this improvement will be to reduce the inclusive learning curve time typically encountered by new BISON users by simplifying input requirements through the use of templates and introducing output automation features.

7. ACKNOWLEDGEMENTS

The authors would like to acknowledge several people that contributed useful information and feedback. Doug Porter and Doug Crawford of the Idaho National Laboratory and Florent Heidet of Argonne National Laboratory all provided essential input parameters and operating conditions that helped model the IFR-1 experiment in BISON. Mark Baird, Paul Miller, and Brandon Langley of Oak Ridge National Laboratory provided technical assistance with computational difficulties.

Portions of this research were funded by the US DOE Office of Nuclear Energy through the VTR project and NEAMS. This research was also supported in part by an appointment to the Oak Ridge National Laboratory NESLS Program, sponsored by the US Department of Energy, and administered by the Oak Ridge Institute for Science and Education.

REFERENCES

1. K. PASAMEHMETOGLU, "Versatile Test Reactor Overview," Idaho National Laboratory, Advanced Reactors Summit VI, San Diego, CA, USA, Jan. 29–31 (2019).
2. R.A. LEFEBVRE et al, *NEAMS Workbench Status and Capabilities,* ORNL/TM-2019/1314, Oak Ridge National Laboratory, September 2019.
3. R. L. WILLIAMSON et al., "Multidimensional Multiphysics Simulation of Nuclear Fuel Behavior," *Journal of Nuclear Materials*, 423 (2012) 149–163.
4. D. L. PORTER, H. TSAI, *Full-length Metallic Fast Reactor Fuel Pin Test in FFTF (IFR-1)*, INL/LTD-11-21062, Idaho National Laboratory, March 2011.
5. D. L. PORTER, H. TSAI, "Full-length U-xPu-10Zr (x = 0, 8, 19 wt. %) fast reactor fuel test in FFTF," *Journal of Nuclear Materials,* 427 (2012) 46–57.
6. A. L. PITNER, R. B. BAKER, "Metal fuel test program in the FFTF," *Journal of Nuclear Materials*, 204 (1993) 124–130.
7. K. M. CUNNINGHAM, J. J. POWERS, R. A. LEFEBVRE, "Modeling the IFR-1 Metal Fuel Experiment in BISON through the NEAMS Workbench," *Transactions of the American Nuclear Society*, ANS Winter Meeting, Washington, D.C., Nov. 17–21 (2019), *in press*.
8. F. H. HUANG, "Fracture Toughness and Tensile Properties of Alloy HT9 in Thin Sections under High Neutron Fluences," Effects of Radiation on Materials: 15th International Symposium, ASTM STP 1125, R. E. Stoller, A. S. Kumar, and D. S. Gelles, Eds., American Society for Testing and Materials, Philadelphia, 1267–1286 (1992).
9. R. A. LEFEBVRE, B. R. LANGLEY, J. P. LEFEBVRE, "Workbench Analysis Sequence Processor," ORNL/TM-2017/619, Oak Ridge National Laboratory, 2017.

APPENDIX A. BISON IFR-1 INPUT FILE

APPENDIX A. BISON IFR-1 INPUT FILE

```
#Documentation
#Version: 010
#Model: Fuel Pin IFR1 from FFTF
#Creation Date: 6/25/2019
#Updated: 8/1/2019
#Edited by: cunninghamkm@ornl.gov
#Notable Changes: Baseline updated & most recent blankets
#removed IFR-1 Input, updated axial peaking factors,
#updated pitch (p/d = 1.19), updated factor

[GlobalParams]
density = 15800.0
order = SECOND
family = LAGRANGE
energy_per_fission = 3.2e-11 # J/fission
volumetric_locking_correction = false
displacements = 'disp_x disp_y'
[]

[Problem]
coord_type = RZ
type = ReferenceResidualProblem
solution_variables = 'disp_x disp_y temp'
reference_residual_variables = 'saved_x saved_y saved_t'
[]

[Mesh]
# rod specific parameters
type = SmearedPelletMesh
clad_thickness = 0.56e-03
pellet_outer_radius = 2.49e-03
pellet_height = 91.4e-02 #no blankets
clad_top_gap_height = 106.2e-02
clad_gap_width = 3.80e-04
top_bot_clad_height = 2.24e-03
clad_bot_gap_height = 3.10e-04
# meshing parameters
clad_mesh_density = customize
pellet_mesh_density = customize
nx_p = 6
ny_p = 260
nx_c = 4
ny_c = 260
ny_cu = 3
ny_cl = 3
```

```
46   pellet_quantity = 1
47   elem_type = QUAD8
48   # mesh options
49   patch_size = 50
50   patch_update_strategy = auto
51   partitioner = centroid
52   centroid_partitioner_direction = y
53   []
54
55   [Variables]
56   [./disp_x]
57   [../]
58   [./disp_y]
59   [../]
60   [./temp]
61   initial_condition = 295
62   [../]
63   []
64
65   [AuxVariables]
66   [./saved_x]
67   [../]
68   [./saved_y]
69   [../]
70   [./saved_t]
71   [../]
72   # Aux variables for output
73   [./porosity]
74   order = CONSTANT
75   family = MONOMIAL
76   [../]
77   [./stress_xx]
78   order = CONSTANT
79   family = MONOMIAL
80   [../]
81   [./stress_yy]
82   order = CONSTANT
83   family = MONOMIAL
84   [../]
85   [./stress_zz]
86   order = CONSTANT
87   family = MONOMIAL
88   [../]
89   [./vonmises]
90   order = CONSTANT
91   family = MONOMIAL
92   [../]
```

```
93   [./hydrostatic_stress]
94   block = pellet
95   order = CONSTANT
96   family = MONOMIAL
97   [../]
98   [./creep_strain_mag]
99   order = CONSTANT
100  family = MONOMIAL
101  [../]
102  [./gap_cond]
103  order = CONSTANT
104  family = MONOMIAL
105  [../]
106  [./coolant_htc]
107  order = CONSTANT
108  family = MONOMIAL
109  [../]
110  [./cumulative_damage_index]
111  order = CONSTANT
112  family = MONOMIAL
113  [../]
114  [./element_failed]
115  order = CONSTANT
116  family = MONOMIAL
117  [../]
118  [./solid_swell]
119  block = pellet
120  order = CONSTANT
121  family = MONOMIAL
122  [../]
123  [./gas_swell]
124  block = pellet
125  order = CONSTANT
126  family = MONOMIAL
127  [../]
128  [./volumetric_strain]
129  block = pellet
130  order = CONSTANT
131  family = MONOMIAL
132  [../]
133  [./hoop_stress]
134  order = CONSTANT
135  family = MONOMIAL
136  [../]
137  [./hoop_creep_strain]
138  order = CONSTANT
139  family = MONOMIAL
```

```
[../]
[./hoop_plastic_strain]
order = CONSTANT
family = MONOMIAL
[../]
[./hoop_elastic_strain]
order = CONSTANT
family = MONOMIAL
[../]
[./total_hoop_strain]
order = CONSTANT
family = MONOMIAL
[../]
[]

[Functions]
[./power_history]
type = PiecewiseLinear
x = '0 3600 2543760 2547360 11904480 11908080 20349360
20352960 26081280 26084880 33472080 33475680 44422560'
y = '0 45723.2 43099.2 40442.4 38212 39819.2 38244.8
35620.8 35620.8 32996.8 29979.2 32144 31684.8'
[../]
[./coolant_press_ramp]
type = PiecewiseLinear
x = '0 3600 2543760 2547360 11904480 11908080 20349360
20352960 26081280 26084880 33472080 33475680 44422560'
y = '0.151e6 0.151e6 0.151e6 0.151e6 0.151e6 0.151e6
0.151e6 0.151e6 0.151e6 0.151e6 0.151e6 0.151e6 0.151e6'
[../]
[./coolant_temp_ramp]
type = PiecewiseLinear
x = '0 3600 2543760 2547360 11904480 11908080 20349360
20352960 26081280 26084880 33472080 33475680 44422560'
y = '298.0 633.0 633.0 633.0 633.0 633.0 633.0 633.0 633.0
633.0 633.0 633.0 350.0'
[../]
[./axial_peaking_factors]
type = PiecewiseBilinear
x = ' 0 0.000821953 0.006975819 0.012518235 0.046227984
0.092200084 0.136933675 0.183506061 0.228848865 0.274791955
0.320110956 0.366033962 0.402767457 0.411950273 0.457244726
0.503146904 0.549038669 0.594921507 0.640184719 0.68605268
0.731309197 0.777781164 0.823030986 0.868889277 0.886005987
0.895152354 0.901245221 0.906724413 0.913433187' # axial
length, 29 points
#1 2 3 4 5 6 7 8 9 10 11 12 13 14 15 16 17 18 19 20 21 22
```

```
187  23 24 25 26 27 28 29
188  y = '0 3600 2543760 2547360 11904480 11908080 20349360
189  20352960 26081280 26084880 33472080 33475680 44422560'
190  #time in seconds, 13 points
191  Z- 29 values for x listed 13 times (y)
192  z = '0 0.49661968 0.5722864 0.64972008 0.74273203
193  0.87965259 0.98312476 1.09186242 1.18828444 1.25652355
194  1.29659156 1.31728199 1.32221131 1.32212284 1.30407578
195  1.27545645 1.22218224 1.14777528 1.05576358 0.94613537
196  0.83827411 0.7092683 0.58555748 0.45303545 0.39475524
197  0.3083747 0.23963428 0.16737763 0.10743662 0 0.49661968
198  0.5722864 0.64972008 0.74273203 0.87965259 0.98312476
199  1.09186242 1.18828444 1.25652355 1.29659156 1.31728199
200  1.32221131 1.32212284 1.30407578 1.27545645 1.22218224
201  1.14777528 1.05576358 0.94613537 0.83827411 0.7092683
202  0.58555748 0.45303545 0.39475524 0.3083747 0.23963428
203  0.16737763 0.10743662 0 0.49661968 0.5722864 0.64972008
204  0.74273203 0.87965259 0.98312476 1.09186242 1.18828444
205  1.25652355 1.29659156 1.31728199 1.32221131 1.32212284
206  1.30407578 1.27545645 1.22218224 1.14777528 1.05576358
207  0.94613537 0.83827411 0.7092683 0.58555748 0.45303545
208  0.39475524 0.3083747 0.23963428 0.16737763 0.10743662 0
209  0.49661968 0.5722864 0.64972008 0.74273203 0.87965259
210  0.98312476 1.09186242 1.18828444 1.25652355 1.29659156
211  1.31728199 1.32221131 1.32212284 1.30407578 1.27545645
212  1.22218224 1.14777528 1.05576358 0.94613537 0.83827411
213  0.7092683 0.58555748 0.45303545 0.39475524 0.3083747
214  0.23963428 0.16737763 0.10743662 0 0.49661968 0.5722864
215  0.64972008 0.74273203 0.87965259 0.98312476 1.09186242
216  1.18828444 1.25652355 1.29659156 1.31728199 1.32221131
217  1.32212284 1.30407578 1.27545645 1.22218224 1.14777528
218  1.05576358 0.94613537 0.83827411 0.7092683 0.58555748
219  0.45303545 0.39475524 0.3083747 0.23963428 0.16737763
220  0.10743662 0 0.49661968 0.5722864 0.64972008 0.74273203
221  0.87965259 0.98312476 1.09186242 1.18828444 1.25652355
222  1.29659156 1.31728199 1.32221131 1.32212284 1.30407578
223  1.27545645 1.22218224 1.14777528 1.05576358 0.94613537
224  0.83827411 0.7092683 0.58555748 0.45303545 0.39475524
225  0.3083747 0.23963428 0.16737763 0.10743662 0 0.49661968
226  0.5722864 0.64972008 0.74273203 0.87965259 0.98312476
227  1.09186242 1.18828444 1.25652355 1.29659156 1.31728199
228  1.32221131 1.32212284 1.30407578 1.27545645 1.22218224
229  1.14777528 1.05576358 0.94613537 0.83827411 0.7092683
230  0.58555748 0.45303545 0.39475524 0.3083747 0.23963428
231  0.16737763 0.10743662 0 0.49661968 0.5722864 0.64972008
232  0.74273203 0.87965259 0.98312476 1.09186242 1.18828444
233  1.25652355 1.29659156 1.31728199 1.32221131 1.32212284
```

```
234  1.30407578 1.27545645 1.22218224 1.14777528 1.05576358
235  0.94613537 0.83827411 0.7092683 0.58555748 0.45303545
236  0.39475524 0.3083747 0.23963428 0.16737763 0.10743662 0
237  0.49661968 0.5722864 0.64972008 0.74273203 0.87965259
238  0.98312476 1.09186242 1.18828444 1.25652355 1.29659156
239  1.31728199 1.32221131 1.32212284 1.30407578 1.27545645
240  1.22218224 1.14777528 1.05576358 0.94613537 0.83827411
241  0.7092683 0.58555748 0.45303545 0.39475524 0.3083747
242  0.23963428 0.16737763 0.10743662 0 0.49661968 0.5722864
243  0.64972008 0.74273203 0.87965259 0.98312476 1.09186242
244  1.18828444 1.25652355 1.29659156 1.31728199 1.32221131
245  1.32212284 1.30407578 1.27545645 1.22218224 1.14777528
246  1.05576358 0.94613537 0.83827411 0.7092683 0.58555748
247  0.45303545 0.39475524 0.3083747 0.23963428 0.16737763
248  0.10743662 0 0.49661968 0.5722864 0.64972008 0.74273203
249  0.87965259 0.98312476 1.09186242 1.18828444 1.25652355
250  1.29659156 1.31728199 1.32221131 1.32212284 1.30407578
251  1.27545645 1.22218224 1.14777528 1.05576358 0.94613537
252  0.83827411 0.7092683 0.58555748 0.45303545 0.39475524
253  0.3083747 0.23963428 0.16737763 0.10743662 0 0.49661968
254  0.5722864 0.64972008 0.74273203 0.87965259 0.98312476
255  1.09186242 1.18828444 1.25652355 1.29659156 1.31728199
256  1.32221131 1.32212284 1.30407578 1.27545645 1.22218224
257  1.14777528 1.05576358 0.94613537 0.83827411 0.7092683
258  0.58555748 0.45303545 0.39475524 0.3083747 0.23963428
259  0.16737763 0.10743662 0 0.49661968 0.5722864 0.64972008
260  0.74273203 0.87965259 0.98312476 1.09186242 1.18828444
261  1.25652355 1.29659156 1.31728199 1.32221131 1.32212284
262  1.30407578 1.27545645 1.22218224 1.14777528 1.05576358
263  0.94613537 0.83827411 0.7092683 0.58555748 0.45303545
264  0.39475524 0.3083747 0.23963428 0.16737763 0.10743662'
265  # group1 group2 group3 group4 group5 group6 group7 group8
266  group9 group10 group11 group12 group 13
267  # 1 2 3 4 5 6 7 8 9 10 11 12 13 14 15 16 17 18 19 20 21 22
268  23 24 25 26 27 28 29
269  axis = 1
270  scale_factor = 1
271
272  [../]
273  []
274
275  [Kernels]
276  # Define kernels for the various terms in the PDE system
277  [./TensorMechanics] #continuum mechanics stress divergence
278  use_displaced_mesh = true #Incremental formulation
279  save_in = 'saved_x saved_y'
280  [../]
```

```
281  [./gravity]
282  type = Gravity
283  variable = disp_y
284  value = -9.81
285  save_in = 'saved_x saved_y'
286  [../]
287  [./heat]
288  type = HeatConduction
289  variable = temp
290  save_in = 'saved_t'
291  [../]
292  [./heat_ie]
293  type = HeatConductionTimeDerivative
294  variable = temp
295  save_in = 'saved_t'
296  [../]
297  [./heat_source]
298  type = FissionRateHeatSource
299  variable = temp
300  fission_rate = 'fission_rate'
301  save_in = 'saved_t'
302  block = pellet
303  [../]
304  []
305
306  [AuxKernels]
307  [./porosity]
308  type = MaterialRealAux
309  property = porosity
310  variable = porosity
311  block = pellet
312  execute_on = timestep_end
313  [../]
314  [./stress_xx]
315  type = RankTwoAux
316  rank_two_tensor = stress
317  variable = stress_xx
318  index_j = 0
319  index_i = 0
320  execute_on = timestep_end
321  [../]
322  [./stress_yy]
323  type = RankTwoAux
324  rank_two_tensor = stress
325  variable = stress_yy
326  index_j = 1
327  index_i = 1
```

```
328  execute_on = timestep_end
329  [../]
330  [./stress_zz]
331  type = RankTwoAux
332  rank_two_tensor = stress
333  variable = stress_zz
334  index_j = 2
335  index_i = 2
336  execute_on = timestep_end
337  [../]
338  [./vonmises]
339  type = RankTwoScalarAux
340  rank_two_tensor = stress
341  variable = vonmises
342  scalar_type = VonMisesStress
343  execute_on = timestep_end
344  [../]
345  [./hydrostatic_stress]
346  type = RankTwoScalarAux
347  rank_two_tensor = stress
348  variable = hydrostatic_stress
349  scalar_type = Hydrostatic
350  execute_on = timestep_end
351  [../]
352  [./creep_strain_mag]
353  type = RankTwoScalarAux
354  block = clad
355  rank_two_tensor = creep_strain
356  variable = creep_strain_mag
357  scalar_type = EffectiveStrain
358  execute_on = timestep_end
359  [../]
360  [./conductance]
361  type = MaterialRealAux
362  property = gap_conductance
363  variable = gap_cond
364  boundary = 10
365  [../]
366  [./cdf_amount]
367  boundary = '1 2 3'
368  type = MaterialRealAux
369  property = cdf_failure
370  variable = cumulative_damage_index
371  [../]
372  [./failed_element]
373  boundary = '1 2 3'
374  type = MaterialRealAux
```

```
375  property = failed
376  variable = element_failed
377  [../]
378  [./gas_swell]
379  type = MaterialRealAux
380  variable = gas_swell
381  property = gas_swelling
382  execute_on = timestep_end
383  [../]
384  [./solid_swell]
385  type = MaterialRealAux
386  variable = solid_swell
387  property = solid_swelling
388  execute_on = timestep_end
389  [../]
390  [./volumetric_strain]
391  type = RankTwoScalarAux
392  rank_two_tensor = total_strain
393  variable = volumetric_strain
394  scalar_type = VolumetricStrain
395  execute_on = timestep_end
396  block = pellet
397  [../]
398  [./hoop_stress]
399  type = RankTwoAux
400  rank_two_tensor = stress
401  variable = hoop_stress
402  index_j = 2
403  index_i = 2
404  execute_on = timestep_end
405  [../]
406  [./hoop_creep_strain]
407  type = RankTwoAux
408  rank_two_tensor = creep_strain
409  variable = hoop_creep_strain
410  index_j = 2
411  index_i = 2
412  execute_on = timestep_end
413  block = clad
414  [../]
415  [./hoop_plastic_strain]
416  type = RankTwoAux
417  rank_two_tensor = creep_strain
418  variable = hoop_plastic_strain
419  index_j = 2
420  index_i = 2
421  execute_on = timestep_end
```

```
422  block = clad
423  [../]
424  [./hoop_elastic_strain]
425  type = RankTwoAux
426  rank_two_tensor = elastic_strain
427  variable = hoop_elastic_strain
428  index_j = 2
429  index_i = 2
430  execute_on = timestep_end
431  block = clad
432  [../]
433  [./total_hoop_strain]
434  type = RankTwoAux
435  rank_two_tensor = total_strain
436  variable = total_hoop_strain
437  index_j = 2
438  index_i = 2
439  execute_on = timestep_end
440  block = clad
441  [../]
442  []
443
444  [Contact]
445  [./pellet_clad_mechanical]
446  master = 5
447  slave = 10
448  penalty = 1e14
449  model = frictionless
450  formulation = kinematic
451  system = constraint
452  normalize_penalty = true
453  tangential_tolerance = 1e-3
454  normal_smoothing_distance = 0.1
455  [../]
456  []
457
458  [ThermalContact]
459  [./thermal_contact]
460  type = GapHeatTransfer
461  variable = temp
462  master = 5
463  slave = 10
464  quadrature = true
465  gap_conductivity = 61.0
466  min_gap = 0.348e-03
467  [../]
468  []
```

```
469
470  [BCs]
471  [./no_x_all]
472  type = DirichletBC
473  variable = disp_x
474  boundary = 12
475  value = 0.0
476  [../]
477  [./no_y_fuel]
478  type = DirichletBC
479  variable = disp_y
480  boundary = 20
481  value = 0.0
482  [../]
483  [./no_y_clad]
484  type = DirichletBC
485  variable = disp_y
486  boundary = 1
487  value = 0.0
488  [../]
489  [./Pressure]
490  [./coolantPressure]
491  boundary = '1 2 3'
492  function = coolant_press_ramp
493  [../]
494  [../]
495  [./PlenumPressure]
496  [./plenumPressure]
497  boundary = 9
498  initial_pressure = 0.084e6 # Pa
499  startup_time = 0
500  R = 8.3143
501  temperature = ave_temp_interior
502  volume = gas_volume
503  output = plenum_pressure
504  material_input = fis_gas_released
505  displacements = 'disp_x disp_y'
506  [../]
507  [../]
508  []
509  [CoolantChannel]
510  [./convective_clad_surface]
511  boundary = '1 2 3'
512  variable = temp
513  inlet_temperature = coolant_temp_ramp
514  inlet_pressure = coolant_press_ramp
515  inlet_massflux = 5261.5 # kg/m^2-sec
```

```
516  coolant_material = sodium
517  rod_diameter = 0.686e-02 # m
518  rod_pitch = 8.23e-03 # m, p/d = 1.19
519  linear_heat_rate = power_history
520  axial_power_profile = axial_peaking_factors
521  subchannel_geometry = triangular
522  [../]
523  []
524
525  [Materials]
526  [./fission_rate]
527  type = UPuZrFissionRate
528  rod_linear_power = power_history
529  axial_power_profile = axial_peaking_factors
530  pellet_radius = 2.49e-03
531  X_Zr = 0.1
532  X_Pu = 0.19
533  block = pellet
534  outputs = all
535  [../]
536  [./burnup]
537  type = UPuZrBurnup
538  X_Zr = 0.1
539  X_Pu = 0.19
540  density = 15800
541  block = pellet
542  outputs = all
543  [../]
544  [./fuel_elasticity_tensor]
545  type = UPuZrElasticityTensor
546  X_Zr = 0.1
547  X_Pu = 0.19
548  block = pellet
549  temperature = temp
550  [../]
551  [./fuel_elastic_stress]
552  type = ComputeMultipleInelasticStress
553  tangent_operator = nonlinear
554  inelastic_models = 'fuel_upuzrcreep'
555  block = pellet
556  [../]
557  [./fuel_upuzrcreep]
558  type = UPuZrCreepUpdate
559  block = pellet
560  temperature = temp
561  [../]
562  [./fuel_strain]
```

```
563  type = ComputeAxisymmetricRZFiniteStrain
564  block = pellet
565  displacements = 'disp_x disp_y'
566  eigenstrain_names = 'fuel_thermal_strain
567  fuel_volumetric_strain'
568  [../]
569  [./fuel_thermal_expansion]
570  type = ComputeThermalExpansionEigenstrain
571  block = pellet
572  thermal_expansion_coeff = 1.18e-5
573  temperature = temp
574  stress_free_temperature = 295.0
575  eigenstrain_name = fuel_thermal_strain
576  [../]
577  [./fuel_volumetric_swelling]
578  type = UPuZrVolumetricSwellingEigenstrain
579  block = pellet
580  temp = temp
581  hydrostatic_stress = 1e6
582  eigenstrain_name = fuel_volumetric_strain
583  [../]
584  [./metal_fuel_thermal]
585  type = ThermalUPuZr
586  block = pellet
587  X_Zr = 0.1
588  X_Pu = 0.19
589  spheat_model = savage
590  thcond_model = lanl
591  temp = temp
592  [../]
593  [./fuel_density]
594  type = Density
595  block = pellet
596  [../]
597  [./Fission_Gas_Release]
598  type = FgrUPuZr
599  block = pellet
600  fission_rate = fission_rate
601  [../]
602  [./clad_elasticity_tensor]
603  type = ComputeIsotropicElasticityTensor
604  youngs_modulus = 1.88e11
605  poissons_ratio = 0.236
606  block = clad
607  [../]
608  [./clad_stress]
609  type = ComputeMultipleInelasticStress
```

```
610  tangent_operator = nonlinear
611  inelastic_models = 'clad_ht9creep'
612  block = clad
613  [../]
614  [./clad_strain]
615  type = ComputeAxisymmetricRZFiniteStrain
616  block = clad
617  displacements = 'disp_x disp_y'
618  eigenstrain_names = 'clad_thermal_eigenstrain'
619  [../]
620  [./fast_flux]
621  type = FastNeutronFlux
622  block = clad
623  factor = 1.0e15
624  [../]
625  [./clad_ht9creep]
626  type = HT9CreepUpdate
627  block = clad
628  temperature = temp
629  [../]
630  [./thermal_expansion]
631  type = ComputeThermalExpansionEigenstrain
632  block = clad
633  thermal_expansion_coeff = 1.2e-5
634  temperature = temp
635  stress_free_temperature = 295.0
636  eigenstrain_name = clad_thermal_eigenstrain
637  [../]
638  [./clad_thermal]
639  type = ThermalHT9
640  block = clad
641  temp = temp
642  [../]
643  [./clad_density]
644  type = Density
645  block = clad
646  density = 7874.0
647  [../]
648  [./longHT9_failure]
649  type = FailureCladHT9
650  boundary = '1 2 3'
651  method = cdf_long
652  temperature = temp
653  hoop_stress = stress_zz # Since 2D-RZ
654  [../]
655  []
656
```

```
[Preconditioning]
[./SMP]
type = SMP
full = true
[../]
[]

[Executioner]
type = Transient
solve_type = 'PJFNK'
petsc_options = '-snes_ksp_ew'
petsc_options_iname = '-pc_type
pc_factor_mat_solver_package -ksp_gmres_restart'
petsc_options_value = 'lu superlu_dist 51'
line_search = 'none'
l_max_its = 60
l_tol = 8e-3
nl_max_its = 40
nl_rel_tol = 5e-4
nl_abs_tol = 1e-7
end_time = 44422560
dtmin = 100
dtmax = 5e5
[./Quadrature]
order = fifth
side_order = seventh
[../]
[./TimeStepper]
type = IterationAdaptiveDT
dt = 1e2
time_t = ' 0 3600 2543760 2547360 11904480 11908080
20349360 20352960 26081280 26084880 33472080 33475680
44422560'
time_dt = '1e2 1e2 1e2 1e2 1e2 1e2 1e2 1e2 1e2 1e2 1e2 1e2
1e2 600'
iteration_window = 4
optimal_iterations = 10
[../]
[]

[Postprocessors]
[./_dt]
type = TimestepSize
[../]
[./num_lin_it]
type = NumLinearIterations
[../]
```

```
704  [./num_nonlin_it]
705  type = NumNonlinearIterations
706  [../]
707  [./tot_lin_it]
708  type = CumulativeValuePostprocessor
709  postprocessor = num_lin_it
710  [../]
711  [./tot_nonlin_it]
712  type = CumulativeValuePostprocessor
713  postprocessor = num_nonlin_it
714  [../]
715  [./alive_time]
716  type = PerfGraphData
717  section_name = Root
718  data_type = TOTAL
719  [../]
720  [./ave_temp_interior]
721  type = SideAverageValue
722  boundary = 9
723  variable = temp
724  execute_on = 'initial linear'
725  [../]
726  [./approx_FCT]
727  type = AverageNodalVariableValue
728  boundary = 12
729  variable = temp
730  [../]
731  [./ave_FST]
732  type = SideAverageValue
733  boundary = 10
734  variable = temp
735  [../]
736  [./ave_CIT]
737  type = SideAverageValue
738  boundary = 5
739  variable = temp
740  [../]
741  [./avg_clad_temp]
742  type = ElementAverageValue
743  variable = temp
744  block = clad
745  [../]
746  [./peak_clad_temp]
747  type = ElementExtremeValue
748  variable = temp
749  value_type = max
750  block = clad
```

```
751  [../]
752  [./peak_fuel_temp]
753  type = ElementExtremeValue
754  variable = temp
755  value_type = max
756  block = pellet
757  [../]
758  [./max_hydro]
759  type = ElementExtremeValue
760  variable = hydrostatic_stress
761  value_type = max
762  block = pellet
763  [../]
764  [./min_hydro]
765  type = ElementExtremeValue
766  variable = hydrostatic_stress
767  value_type = min
768  block = pellet
769  [../]
770  [./peak_porosity]
771  type = ElementExtremeValue
772  variable = porosity
773  value_type = max
774  block = pellet
775  [../]
776  [./clad_inner_vol]
777  type = InternalVolume
778  boundary = 7
779  [../]
780  [./pellet_volume]
781  type = InternalVolume
782  boundary = 8
783  [../]
784  [./gas_volume]
785  type = InternalVolume
786  boundary = 9
787  execute_on = 'initial timestep_end'
788  [../]
789  [./clad_fuel_gap]
790  type = NodalMaxValue
791  variable = penetration
792  boundary = 10
793  [../]
794  [./flux_from_clad]
795  type = SideFluxIntegral
796  variable = temp
797  boundary = 5
```

```
798  diffusivity = thermal_conductivity
799  [../]
800  [./flux_from_fuel]
801  type = SideFluxIntegral
802  variable = temp
803  boundary = 10
804  diffusivity = thermal_conductivity
805  [../]
806  [./rod_integral_power]
807  type = ElementIntegralPower
808  variable = temp
809  use_material_fission_rate = true
810  fission_rate_material = fission_rate
811  block = pellet
812  [../]
813  [./rod_input_power]
814  type = FunctionValuePostprocessor
815  function = power_history
816  scale_factor = 91.4e-02
817  [../]
818  [./average_burnup]
819  type = ElementAverageValue
820  block = pellet
821  variable = burnup
822  [../]
823  [./max_cdf]
824  type = ElementExtremeValue
825  value_type = max
826  variable = cumulative_damage_index
827  [../]
828  [./fis_gas_produced]
829  type = ElementIntegralFisGasProduce
830  block = pellet
831  [../]
832  [./fis_gas_released]
833  type = ElementIntegralFisGasRelease
834  block = pellet
835  execute_on = 'initial timestep_end'
836  [../]
837  [./creep_timestep]
838  type = MaterialTimeStepPostprocessor
839  block = pellet
840  [../]
841  [./disp_x_9076]
842  type = NodalVariableValue
843  nodeid = 9075
844  variable = disp_x
```

```
  [../]
  [./disp_y_9076]
  type = NodalVariableValue
  nodeid = 9075
  variable = disp_y
  [../]
  [./hydrostatic_stress]
  type = ElementAverageValue
  variable = hydrostatic_stress
  execute_on = 'initial timestep_end'
  block = pellet
  [../]
  [./solid_swelling]
  type = ElementAverageValue
  variable = solid_swell
  block = pellet
  [../]
  [./gas_swelling]
  type = ElementAverageValue
  variable = gas_swell
  block = pellet
  [../]
  [./volumetric_strain]
  type = ElementAverageValue
  variable = volumetric_strain
  block = pellet
  [../]
  [./porosity]
  type = ElementAverageValue
  variable = porosity
  block = pellet
  [../]
  [./fis_gas_percent]
  type = FGRPercent
  value1 = fis_gas_released
  value2 = fis_gas_produced
  [../]
  [./max_cladding_creep_strain]
  type = ElementExtremeValue
  variable = creep_strain_mag
  block = clad
  [../]
  []

  [VectorPostprocessors]
  [./clad_total_hoop_strain]
  type = LineValueSampler
```

```
892  variable = total_hoop_strain
893  start_point = '2.87e-3 2.25e-3 0.0'
894  end_point = '2.87e-3 91.4e-02 0.0'
895  num_points = 200
896  sort_by = y
897  outputs = 'vec'
898  [../]
899  []
900  [Outputs]
901  color = true
902  exodus = true
903  perf_graph = true
904  csv = true
905  [./console]
906  type = Console
907  max_rows = 25
908  interval = 1
909  output_linear = true
910  [../]
911  [./vec]
912  type = CSV
913  execute_on = 'FINAL'
914  file_base = IFR1_br_006_final
915  [../]
916  [./checkfile]
917  type = CSV
918  execute_on = 'FINAL'
919  show = 'max_cladding_creep_strain'
920  [../]
921  []
922
923  [Debug]
924  show_var_residual = 'disp_x disp_y temp'
925  show_var_residual_norms = true
926  []
```